Colloid Polym Sci (2004) 282: 910–917
DOI 10.1007/s00396-004-1129-9

ORIGINAL CONTRIBUTION

**A. Jusufi**
**C. N. Likos**
**M. Ballauff**

# Counterion distributions and effective interactions of spherical polyelectrolyte brushes

Received: 12 February 2004
Accepted: 5 April 2004

A. Jusufi · M. Ballauff (✉)
Physikalische Chemie I,
Universität Bayreuth, 95440 Bayreuth,
Germany
E-mail: matthias.ballauff@uni-bayreuth.de

C. N. Likos
Theoretische Physik II,
Heinrich-Heine-Universität Düsseldorf,
Universitätsstr. 1, 40225 Düsseldorf,
Germany

**Abstract** We consider the electrosteric repulsion of colloidal particles whose surface carries a dense layer of long polyelectrolyte chains (“spherical polyelectrolyte brushes”). The theory of electrosteric repulsion of star polyelectrolytes developed recently is augmented to include particles with a finite core radius. It is shown that most of the counterions are confined within the brush layer. The strong osmotic pressure thus created within the brush layer dominates the repulsive interaction between two such particles. Because of this the pair interaction potential between spherical polyelectrolyte brushes can be given in terms of an analytic expression. The theoretical predictions are compared with available experimental data and semi-quantitative agreement between the two is found.

## Introduction

Colloidal particles are often stabilized by a dense layer of linear chains grafted on their surface [1]. If two particles modified in this way approach each other, the respective surface layers overlap. Hence, the polymer chains of the two particles start to interact. This leads to a repulsive interaction between the particles that is now termed “steric interaction” [2]. The repulsion induced in this way is independent of the salt concentration present in this system. In contrast with the classical DLVO interaction, the steric interaction is therefore operative under conditions where electrostatic repulsions fail to provide sufficient stability against flocculation, e.g. if divalent salt is present. The great industrial importance for the stabilization of, e.g., latex particles is directly evident and has led to a large body of papers on this subject. The older work devoted to steric stabilization is well summarized in the treatise of Napper [3] while more recent citations can be found in the classical book of Israelachvili [4].

E.W. Fischer in 1958 was the first to develop a quantitative theory of steric stabilization of spherical particles [5]. In his seminal paper he calculated the increase of free energy induced by the overlapping of the two polymer layers of the approaching particles. The repulsive interaction between the two particles is recast in terms of the osmotic pressure in the lens-shaped overlap volume. The osmotic pressure, in turn, is calculated by use of the second virial coefficient of polymer solutions assuming a constant polymer density within the overlap volume. This approach also enables introduction of solvent power into the theory. The Fischer theory therefore can fully explain the mechanism of steric stabilization in a good solvent, as well as the onset of attractive interactions if the surrounding medium is a poor solvent for the polymer chains grafted to the surface of the particles (see the discussion of this point in the treatise of Napper [3]).

The Fischer theory is among the most successful approaches of modern colloid science. It has been further developed and the number of publications devoted to steric interaction related to this theory is hard to overlook. For a survey of the literature the reader is deferred to the treatises of Napper [3], and Israelachvili [4], or of Fleer and coworkers [6].

An interesting question that is discussed in the treatise of Napper is overlap of the chains (Section 12.4 of Ref. [3]). Here the chains of the two layers can either occupy the same volume as assumed in Fischer's theory or retract from each other. The latter process referred to as "denting" has been extensively discussed by Napper and rejected [3]. A direct experimental proof of this conjecture has not been given, however. Going through the literature, one gets the impression that the theory of steric repulsion in colloid science that started with Fischer's paper is mostly thought to be complete.

Recently, this picture has changed substantially, however. With the advent of computer simulation the interaction of polymer chains in solution can now be investigated directly. The results of these simulations can be used directly for comprehensive checking of current analytical theory. Charges can also be introduced in these simulations, and then the simulations lead to the effective pair potential of the interacting polymeric objects. This has been demonstrated by considering the interaction of two uncharged star polymers in solution. Some years ago, and based on the original ideas of Witten and Pincus [7], Likos et al. derived an analytical formula for effective interaction between two star polymers showing thereby that this effective potential is ultrasoft, a finding corroborated by experimental work performed by small-angle neutron scattering [8]. Monomer-resolved computer simulations of two interacting star polymers fully confirmed the theoretical predictions [9]. Moreover, subsequent theoretical work demonstrated that the ultrasoft interaction leads to ordered phases if the concentration of the star polymer is raised [10]. An interesting point directly visible in these simulations is the retraction of the arms when two stars approach each other. The virtually unlimited power of simulations for closer understanding of steric interaction has thus become directly obvious.

Recently, this work has been extended to include charged star polymers [11, 12]. By combining molecular dynamics (MD) computer simulations with analytical theory it has been demonstrated that in strongly charged star polymers, the chains assume a rodlike, stretched configuration. This finding has been confirmed on similar brush systems by recent anomalous X-ray small-angle (ASAXS) scattering experiments [13]. Moreover, it has been found that the vast majority of the counterions are absorbed within the corona of the polyelectrolyte stars and give rise to an effective osmotic interaction between them that is, again, ultrasoft in nature but stronger than its counterpart for neutral star polymers [12].

Here we wish to extend this work to include spherical polyelectrolyte brushes, an example of which is schematically depicted in Fig. 1 [14, 15]. The purpose of this paper is twofold. First, we present a theory for the interaction of spherical polyelectrolyte brushes with their counterions. Here the problem of counterion confinement within the brush layer is considered, with emphasis on calculation of the fraction of counterions that are confined within the height of the spherical brush. Subsequently, the effective interaction potential of spherical polyelectrolyte brushes is explicitly calculated and it is shown that, with the approximation of neglecting the number of untrapped counterions, the effective interaction potential assumes an analytical form. In this way the original idea of Fischer [5], namely the interrelation of the osmotic pressure and the repulsive interaction, is expanded to include charged particles.

## Spherical polyelectrolyte brushes: theory

In this section, we put forward a theoretical treatment of isolated spherical polyelectrolyte brushes (PE-brushes), pertaining physically to situations arising in dilute solutions of the brushes. The theory proceeds along lines similar to that developed for star-branched polyelectrolyte systems (PE-stars), presented elsewhere [11, 12]. The main difference from the stars is that the brush thickness $L$ and the core radius $R_c$ have similar sizes, whereas for PE-stars $R_c \to 0$. The core usually consists of a solid latex particle (e.g. polystyrene) with a radius between 50 nm and 100 nm, whereas the brush consists of linear polyelectrolyte chains (e.g. poly(acrylic acid) or poly(styrene sulfonic acid); [14]). Experimental realizations of PE-brushes have been presented elsewhere [14,

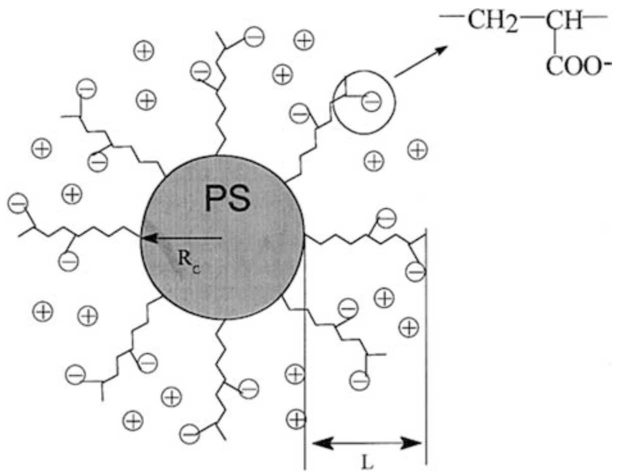

**Fig. 1** A sketch of the spherical polyelectrolyte brush used in the experimental study of Refs. [14, 15]

15]. The counterions (e.g. $Na^+$) are dissolved in the solution and provide the necessary overall charge neutrality.

We start with the description of the theoretical approach for a single PE-brush, which is based on a cell model. Klein Wolterink et al. have introduced this approach for conformational analysis for an isolated polyelectrolyte star, in order to calculate the star radius and its effective charge of the star object, assuming homogeneous charge distribution inside the star [16]. The aforementioned conformational quantities have been obtained by introducing a variational free energy for the system and minimizing it with respect to these quantities. The model has been modified by assuming fully stretched chains (inhomogeneous density profile inside the star) and by taking into account the cylindrical counterion condensation along the stretched chains [11]. The distinction of the counterion density distribution states has led to very good agreement of the theory with simulation results [12].

## An isolated PE-brush

We extend the theory of the PE-stars to PE-brushes in a cell model and make use of some aspects of the star model as studied in Ref. [12]. For the sake of simplicity, we do not treat the brush thickness $L$ as a varying property and limit ourselves to the question of counterion partition between free and trapped ones.

An isolated PE-brush can be considered as a neutral solid core with grafted chains on its surface. The properties are determined according to the physical conditions, as described in detail in Ref. [14]. The cell radius (Wigner–Seitz radius) $R_W$ is determined by the concentration $c$ of PE-brushes in the solution via the relationship $c = 3/\left(4\pi R_W^3\right)$. In accordance to the experimental conditions, we vary $R_W$ in the range $600\ \mathrm{nm} \leq R_W \leq 1100\ \mathrm{nm}$. The bare charge is roughly $Q_{\mathrm{bare}} = 6\times10^5|e|$, where $e$ denotes the elementary charge. The experimental values for brush thickness and core radius are $L = 67$ mm and $R_c = 68$ nm, respectively. Because $R_W > > R_c + L$, the average interbrush distance greatly exceeds the typical size of the particles and thus the model describes a dilute solution of spherical PE-brushes. Figure 2 illustrates the geometry of the cell model and the physical situation.

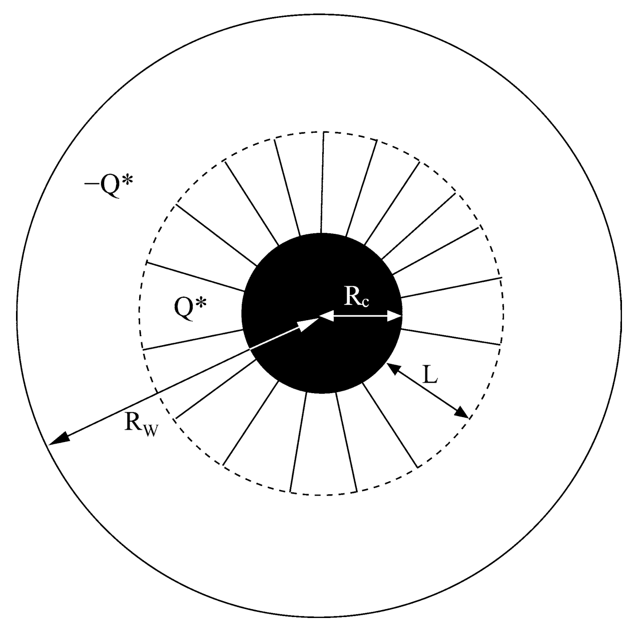

**Fig. 2** A sketch of a spherical polyelectrolyte brush in its Wigner–Seitz cell. The chains are represented by lines and are grafted on the core surface (*filled sphere in the center*). The spherical particle is enclosed in a cell of radius $R_W$ and carries the net charge $Q^*$

Because the grafted polyelectrolytes carry a very high charge (almost every monomer along the chain is charged), we expect a significant number of counterions to be cylindrically condensed along the rodlike chains. A simple estimate of the number of condensed counterions can be obtained by considering the Manning parameter, $\xi$ [17, 18, 19, 20, 21, 22], which is defined as the ratio of the Bjerrum length $\lambda_B = e^2/(\epsilon k_B T)$ (where $\epsilon$ denotes the dielectric constant of the solvent, $k_B$ is Boltzmann's constant, and $T$ is the absolute temperature) to the distance $a$ between two sequential charged sites. With the Bjerrum length $\lambda_B = 7.1$ Å (corresponding to water at room temperature), we obtain for the Manning parameter the value $\xi = (\lambda_B/a) \approx 3$. This implies that the number of condensed counterions is $Q_{\mathrm{cond}} = Q_{\mathrm{bare}}(1-1/\xi)$, approximately two-thirds of the bare charge. Therefore the effective charge is $Q = Q_{\mathrm{bare}} - Q_{\mathrm{cond}} = 2\times10^5|e|$. Because the chains are stiff, we assume that the charge distribution $\rho(r)$ decays with $r^{-2}$ within the PE-brush, where $r$ stands for the distance from the core center. This assumption is justified both by simulation results for PE-stars [11, 12] and by recent anomalous small-angle X-ray scattering (ASAXS) experiments on PE-brushes [13].

We consider first the quantity commonly referred to as the *osmotic coefficient*, defined as $\Phi = \Pi/\Pi_{\mathrm{id}}$, where $\Pi$ is the osmotic pressure of the solution and $\Pi_{\mathrm{id}}$ is the ideal osmotic pressure arising from a solution of all the counterions of the solution, assumed to be interacting neither with themselves nor with the macro ion. The osmotic pressure $\Pi$ can be measured by osmometry [15]. In principle, there are two contributions to $\Pi$, one arising from the free counterions in the solution and one arising from the spherical particles themselves. However, in a dilute solution the contribution from the brushes is dominated by the ideal part, which is proportional to the brush concentration $c$. Because every brush releases an enormous number of counterions, the concentration of the latter is much higher than that of the brushes and hence the brush contribution to the osmotic pressure can be neglected. On the other hand, it is only the free counterions that contribute to the osmotic pressure, thus the osmotic coefficient $\Phi$ is simply equal to the ratio between the free counterions and the total number of counterions. The number of free counterions is, in turn, equal to $Q^*/|e|$, where $Q^*$ is the net charge of the brush that remains after the charge of the absorbed counterions has been subtracted. Therefore the osmotic coefficient is given as:

$$\Phi = \frac{Q^*}{Q_{\mathrm{bare}}} \tag{1}$$

and calculation of the osmotic coefficient reduces to determination of $Q^*$.

The equilibrium value for the net charge $Q^*$ is determined by minimization of a variational free energy $F(Q^*)$, which we write as:

$$F(Q^*) = U_{\mathrm{H}} + S_{\mathrm{in}} + S_{\mathrm{out}} \tag{2}$$

where $U_{\mathrm{H}}$ is the electrostatic contribution, and $S_{\mathrm{in}}$ and $S_{\mathrm{out}}$ are entropic contributions from the counterions inside the brush and outside the brush, respectively. We have neglected any elastic or self-avoidance terms, because these do not depend on $Q^*$ and drop out after taking the derivative of $F(Q^*)$ with respect to $Q^*$.

The term $U_{\mathrm{H}}$ is the Hartree-type, mean-field electrostatic energy of the whole brush:

$$U_{\mathrm{H}} = \frac{1}{2\varepsilon}\int\!\!\int d^3r\, d^3r' \frac{\varrho(\mathbf{r})\varrho(\mathbf{r}')}{|\mathbf{r}-\mathbf{r}'|} \tag{3}$$

with the local *charge* density $\varrho(\mathbf{r})$ to be defined. Because the chains are modeled as being fully stretched, the density distributions inside the brush fall off as $\sim r^{-2}$ from the core surface. On the other hand, the charge distribution outside the brush arises from the presence of free counterions there, which we model as having uniform density. Accordingly, we write:

$$\begin{aligned}\frac{\varrho(\mathbf{r})}{Q^*} = &\frac{\Theta(R_{\mathrm{c}}+L-r)\Theta(r-R_{\mathrm{c}})}{4\pi L r^2} \\ &- \frac{\Theta(r-R_{\mathrm{c}}-L)\Theta(R_{\mathrm{W}}-r)}{V(R_{\mathrm{W}})-V(R_{\mathrm{c}}+L)}\end{aligned} \tag{4}$$

with the volume $V(z) = 4\pi z^3/3$ of a sphere of radius $z$ and the Heaviside step function $\Theta(x)$. It is straightforward to see that $\varrho(\mathbf{r})$ integrates to zero within the Wigner–Seitz cell, thus electroneutrality is guaranteed. At this point we distinguish the number of counterions inside the brush as $N_{\mathrm{in}} = (Q-Q^*)/|e|$ and the free ones outside the brush, $N_{\mathrm{out}} = Q^*/|e|$. We thus obtain the electrostatic energy as:

$$\frac{U_{\mathrm{H}}}{k_{\mathrm{B}}T} = \frac{N_{\mathrm{in}}^2\lambda_{\mathrm{B}}}{2} \times \left[\frac{R_{\mathrm{c}}}{L^2}\vartheta_{\mathrm{in}}\left(\frac{R_{\mathrm{c}}+L}{R_{\mathrm{c}}}\right) + \frac{1}{R_{\mathrm{c}}+L}\vartheta_{\mathrm{out}}\left(\frac{R_{\mathrm{c}}+L}{R_{\mathrm{W}}}\right)\right] \tag{5}$$

where the functions $\vartheta_i\,(x)$ ($i$ = in, out) are given by:

$$\begin{aligned}\vartheta_{\mathrm{in}}(x) &= x - 2ln(x) - \frac{1}{x} \\ \vartheta_{\mathrm{out}}(x) &= \frac{5-9x+5x^3-x^6}{5(1-x^3)^2}\end{aligned}$$

The ideal entropic contributions $S_i$ ($i$ = in, out) arising from the counterions are of the form:

$$\frac{S_i}{k_{\mathrm{B}}T} = \int_{V_i} d^3r\, \rho_i(r)\left[ln\left(\rho_i(r)a^3\right) - 1\right] + 3N_i ln\left(\frac{\Lambda}{a}\right) \tag{6}$$

where $\rho_i\,(r) = N_i/V_i$ are the *number* densities of the counterions in the two different volume regimes $V_i$, according to the charge distribution in Eq. (4). In Eq. (6) above, $\Lambda$ is the thermal de Broglie wavelength of the counterions. In writing the sum of the entropic contributions in Eq. (2), the terms $3N_i$ ln $(\Lambda/a)$ will be dropped in what follows, because they add up to the irrelevant constant $3(Q/|e|)\ln(\Lambda/a)$.

The functional form of the number densities $\rho_i(r)$ needs to be specified. Because the trapped counterions follow the profile of the charged monomers, we write $\rho_{\mathrm{in}}(r) = Cr^{-2}\Theta(R_{\mathrm{c}}+L-r)\Theta(r-R_{\mathrm{c}})$. Outside the brush, we have a uniform distribution of the free counterions within the cell $R_{\mathrm{c}}+L<r<R_{\mathrm{W}}$, thus we write $\rho_{\mathrm{out}}(r) = \Theta(r-R_{\mathrm{c}}-L)\Theta(R_{\mathrm{W}}-r)N_{\mathrm{out}}/V_{\mathrm{out}}$, with $V_{\mathrm{out}} = V(R_{\mathrm{W}}) - V(R_{\mathrm{c}}+L)$. Carrying out the integrations in Eq. (6), we obtain the following expressions for the entropic contributions of the counterions in their two different states:

$$\frac{S_{\mathrm{in}}}{k_{\mathrm{B}}T} = N_{\mathrm{in}}\left[1 + ln\left(\frac{N_{\mathrm{in}}a^3}{4\pi L(R_{\mathrm{c}}+L)^2}\right) - 2\frac{R_{\mathrm{c}}}{L}ln\left(\frac{R_{\mathrm{c}}+L}{R_{\mathrm{c}}}\right)\right] \tag{7}$$

$$\frac{S_{\mathrm{out}}}{k_{\mathrm{B}}T} = N_{\mathrm{out}}\left[ln\left(\frac{N_{\mathrm{out}}a^3}{V(R_{\mathrm{W}})-V(R_{\mathrm{c}}+L)}\right) - 1\right] \tag{8}$$

The value $Q^*$ is found by minimization of the free energy, Eq. (2). The final result is:

$$\begin{aligned}\frac{Q^*}{|e|} = &-\frac{1}{\lambda_{\mathrm{B}}} \\ &\times\left[\frac{R_{\mathrm{c}}}{L^2}\vartheta_{\mathrm{in}}\left(\frac{R_{\mathrm{c}}+L}{R_{\mathrm{c}}}\right) + \frac{1}{R_{\mathrm{c}}+L}\vartheta_{\mathrm{out}}\left(\frac{R_{\mathrm{c}}+L}{R_{\mathrm{W}}}\right)\right]^{-1} \\ &\times\left[-2 + 2\frac{R_{\mathrm{c}}}{L}ln\left(\frac{R_{\mathrm{c}}+L}{R_{\mathrm{c}}}\right)\right. \\ &\left. + ln\left(\frac{Q^*}{Q-Q^*}\frac{4\pi L(R_{\mathrm{c}}+L)^2}{V(R_{\mathrm{W}})-V(R_{\mathrm{c}}+L)}\right)\right]\end{aligned} \tag{9}$$

$Q^*$ carries an explicit density-dependence through the Wigner–Seitz radius $R_{\mathrm{W}}$, a usual situation for charged

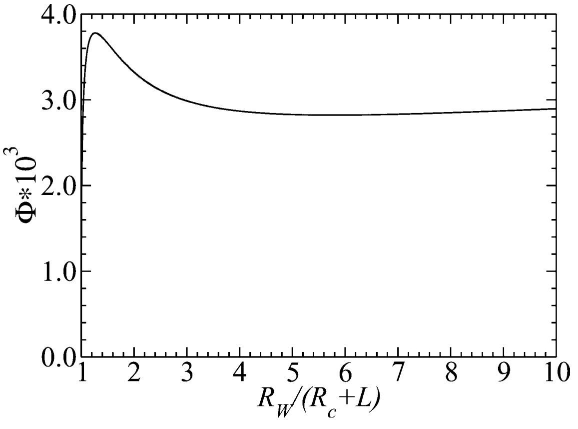

**Fig. 3** The osmotic coefficient $\Phi$ as a function of the cell radius $R_W$. The parameters used stem from experimental values: effective charge $Q = 2.1\times10^5|e|$, $\xi = 3.5$, core radius $R_c = 68$ nm, brush thickness $L = 67$ nm

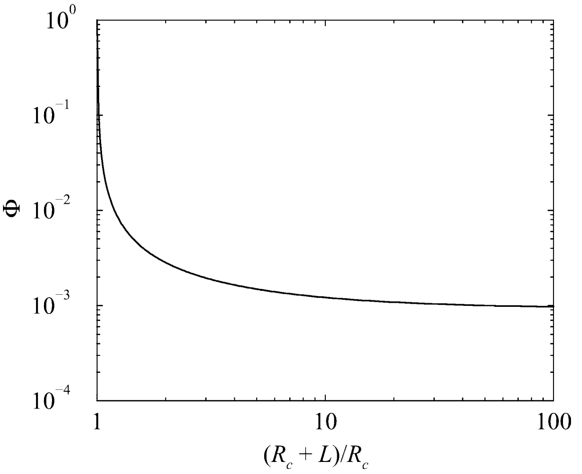

**Fig. 4** The osmotic coefficient $\Phi$ as a function of the brush thickness $L$. For a detailed description of the parameters used and the way the ratio $(R_c + L)/R_c$ was varied, see the text

systems, familiar from the statistical mechanics of charged-stabilized colloids also [23].

The dependence of the osmotic coefficient $\Phi$ on the concentration is shown in Fig. 3. In contrast, the charges of the PE-stars are more sensitive to changes of the cell radius $R_W$. First we note that the absolute scale of the coefficient is two orders of magnitude smaller than that obtained for the PE-stars, for which typical values of 0.15–0.30 for the osmotic coefficient were obtained [12]. This is a consequence of the much higher bare charge carried by the brushes, which exerts a strong electrostatic attraction on the counterions and pulls them back into the interior of the brush. The experimental values for PE-brushes lie in the range $\Phi = 0.02$–$0.05$ [15], i.e. they are also much smaller than for PE-stars.

Although our theory correctly predicts the reduction of the osmotic coefficient in brushes as compared with stars, the theoretical values are still too low, roughly one order of magnitude smaller than the experimental values [15]. The source of this discrepancy most probably lies in the mean-field character of the electrostatic part of our theory, i.e. neglecting the lateral chain fluctuations that can polarize the core. Work on improving the theory along these lines in currently in progress. Still, within the limitations of our mean-field approach, certain trends and characteristics of the theory are in agreement with experimental observations.

One agreement of our theory with experimental results is the weak dependence of $\Phi$ with varying brush concentration, (varying the cell radius $R_W$), as can be seen in Fig. 3 [15]. In the limit $R_W \to R_c + L$ (overlap concentration $c^*$), there is no longer any free space for the counterions and the osmotic coefficient approaches zero: all counterions are absorbed. On reducing the concentration, $\Phi$ grows and attains a local maximum at about $R_W/(R_c + \mathrm{L}) \cong 1.2$. The origin of this maximum probably lies in the assumption of uniform counterion density profiles outside the brush, whose validity becomes questionable for concentrations approaching $c^*$. Upon further decrease of the concentration $c \sim R_W^{-3}$over about two orders of magnitude $(2 < R_W/(R_c + L) < 10)$, the osmotic coefficient remains roughly constant, in full agreement with experimental observations [15].

Let us now discuss the dependence of $\Phi$ on the relative brush thickness $L$ compared with the extent of the rigid core $R_c$. We have determined the linear charge density $\lambda$ of the experimental PE-brush as $\lambda = Q/L = 2.1\times10^5|e|/670\text{Å}^{-1} \cong 313|e|/\text{Å}$ and then we varied the brush thickness $L$ and the charge $Q$ in Eq. (9) as $Q = \lambda \mathrm{L}$, solving this equation self-consistently for $Q^*$. The core radius was kept fixed at the experimental value $R_c = 68$ nm and $L$ was varied in such a way that the ratio $(R_c + L)/R_c$ spanned the range from 1 to 100. The ratio of the Wigner–Seitz radius $R_W$ to the total extent of the core and the brush was thereby fixed at the value $R_W = 8.15(R_c + L)$ and the dependence of $\Phi$ on the height of the brush was monitored. The result is shown in Fig. 4. In the limit of vanishing brush thickness, $(R_c + L)/R_c \to 1$, the osmotic coefficient approaches unity, because there is no longer any brush and thus all counterions are free. There is a dramatic decrease of $\Phi$ with increasing brush thickness, however, and values of $\Phi$ of order $10^{-3}$ are rapidly reached. This demonstrates the ability of PE-brushes to capture the vast majority of the counterions even at moderate brush heights, $L \cong R_c$.

## Effective interaction between two spherical PE-brushes

An important tool in understanding quantitatively the structural correlations of spherical PE-brushes and the phase behavior of the brushes is the concept of effective interactions between two of those objects [24]. We will employ a first calculation of this important quantity and give only an outline in what follows. The theoretical picture of the model is based on the idea already carried out for overlapping PE-stars [11, 12]. Under these conditions, the chains from each of the two spherical brushes retract [12] and they can be modeled as "chopped spheres" (Fig. 5). To corroborate this picture, we show in Fig. 6 a simulation snapshot of two PE-stars at small separations $D$, as was shown in Ref. [12]. The retraction of the chains towards the half-space belonging to the respective cores is an essential ingredient of the theory and it is at odds with the picture of mutually overlapping chains. Nevertheless, extensive computer simulations both of neutral [9] and of charged star polymers [11, 12] show beyond doubt that the chains of each star retract, a condition known as *no interdigitation*. Hence, the question of "denting" discussed many years ago by Napper [3] is now resolved. The no-interdigitation condition is also an important ingredient in the theoretical analysis of the effective forces between planar polymer brushes [25, 26, 27] and also plays a central role in the arguments put forward by Pincus [28] regarding the force between neutral and charged spherical brushes.

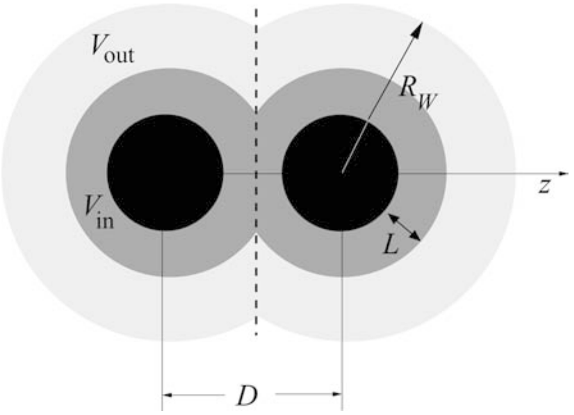

**Fig. 5** A sketch of two polyelectrolyte-brushes of core radius $R_c$ (*black center spheres*) each, held at center-to-center separation $D$. The dark fused spheres denote the brush regime of thickness $L$ and have a total volume $V_{in}$. The light "eight-shaped" hollow region of volume $V_{out}$ denotes the region in which the free counterions can move

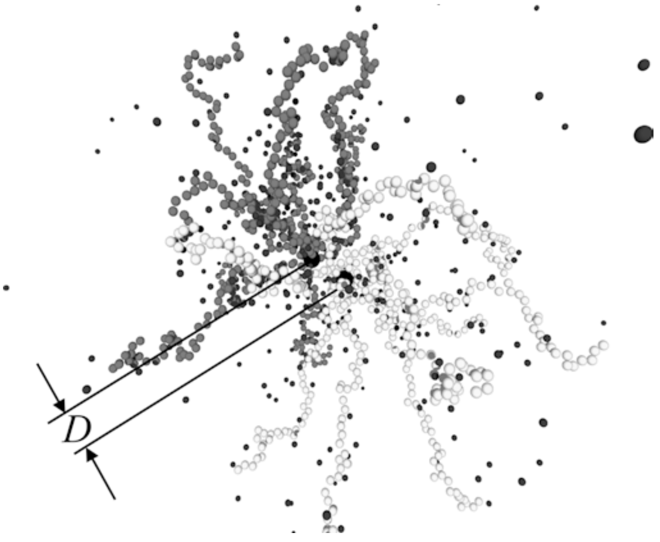

**Fig. 6** A simulation snapshot of two 10-arm PE-stars at small separations $D$ (taken from Ref. [12])

The effective interaction $V_{eff}(D)$ between two spherical PE brushes, kept at center-to-center distance $D$, results after taking a canonical trace over all but the core-centers degrees of freedom and is defined as:

$$V_{eff}(D) = F_2(D) - F_2(\infty) \tag{10}$$

where $F_2(z)$ is the Helmholtz free energy of two PE brushes at center-to-center separation $z$ [24]. because two spherical brushes at infinite separation experience no influence from one another, the term $F_2\,(\infty)$ is simply twice the free energy of an isolated brush, as calculated in the section "An isolated PE-brush". The procedure for theoretical calculation of the effective interaction remains the same as for PE-stars [12]. Based on the results of the preceding section, we can simplify our calculations by neglecting the tiny fraction of charge outside of the brush, because $\Phi$ is very small. In such circumstances, the local charge density $\varrho(r)$ vanishes identically and the electrostatic contribution $U_H$ can be dropped. The dominant term arises from the entropic contribution of the counterions inside the brushes. Then, the effective interaction stems from the difference between the entropic term $S_{in}(D)$ of the trapped counterions when the brush centers are kept at finite distance $D$ and the contribution $S_{in}(\infty)$ of two isolated spherical brushes:

$$V_{eff}(D) = S_{in}(D) - S_{in}(\infty) \tag{11}$$

The calculation of the term $S_{in}(D)$ under the conditions of $\sim r^{-2}$ density profiles and of no-interdigitation follows lines similar to those presented in Ref. [12], but taking explicitly into account the vanishing density inside the cores. The final result can be cast in an analytical form and reads as:

$$\begin{aligned}\frac{V_{eff}(D)}{k_BT} = \frac{Q}{|e|}\Bigg[&\frac{1}{2RK}\left(Dln^2\left(\frac{D}{2R}\right)+8R_c ln\left(\frac{R_c}{R}\right)\right)\\ &+ln\left(\frac{2L}{RK}\right)-2\frac{R_c}{L}ln\left(\frac{R_c}{R}\right)\Bigg]\end{aligned} \tag{12}$$

where $R = R_c + L$ and $K$ is a $D$-dependent dimensionless parameter obtained from the condition $\int_{V_{in}}\rho(r)\mathrm{d}^3r = Q$, where $\rho(r) = \mathrm{A}/r^2$ and the normalization factor $A = Q/(4\pi\mathrm{RK})$. This yields:

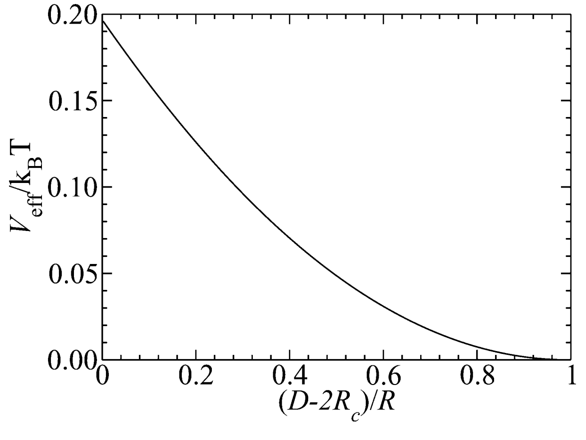

**Fig. 7** The effective pair potential between two spherical PE-brushes per unit counterion ($Q/|e|=1$), as obtained from the analytical expression, Eq. (12), of the text

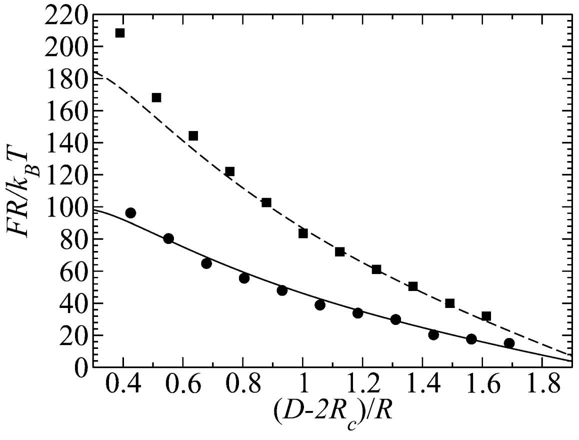

**Fig. 8** The effective force between two PE-stars with $Q=100$ (*solid line*) and $Q=192$ (*dashed line*). The symbols denote simulation results

$$K = 1 - 2\frac{R_c}{R} + \frac{D}{2R}\left[1 - ln\left(\frac{D}{2R}\right)\right] \tag{13}$$

The analytical expression of Eq. (12) is plotted in Fig. 7 per *unit counterion*, $Q/|e|=1$. As can be seen from this figure, one obtains an ultrasoft interaction. The energy scale is determined by the number of trapped counterions $Q/|e|$ which appears only as a prefactor in Eq. (12). The assertion that the effective interaction is dominated by the entropic contribution of the trapped counterions was first put forward by Pincus [28], who subsequently applied simple scaling arguments to reach the conclusion that the effective interaction has the form of a "ramp" potential. Our findings are in line with Pincus' *physical* assumption of the dominant role of the trapped counterions. On a quantitative basis, however, the effective potential does not have a linear form. The discrepancy between Pincus' results and those presented here is because of the inhomogeneous counterion distribution employed in this model.

To provide further corroboration of the validity of the procedure of ignoring the electrostatic contributions and focusing exclusively on the entropic terms of the trapped counterions, we also applied the same procedure for PE-stars ($R_c \to 0$), for which MD simulation data for the effective force are readily available [12]. As a matter of fact, because the osmotic coefficient for the PE-stars are higher, abandonment of electrostatic contributions in Eq. (10) is less justified than for the PE-brushes, hence our comparison provides a strong test.

As can be seen from Fig. 8, the presented approach gives a very good description even for PE-stars. The data shown correspond to two 10-arm stars with $Q=100$, $R_c=0.04R$, and two 18-arm stars with $Q=192$; $R_c=0.05R$ in this case. We repeat that the quoted $Q$-values are effective charge numbers, i.e. the cylindrically condensed counterions along the rodlike chains are subtracted by using the simple estimate $\xi=3$, as described in the previous section.

The presented approach works very well over a large overlap-separation domain $D$. Only for smaller distances corrections are required and we need to take into account the electrostatic contributions and employ a more detailed calculation, as carried out in Ref. [12]. Nevertheless, the effective pair potential Eq. (12) can be used for PE-stars and spherical PE-brush solutions and provides a manageable analytical expression with the use of which structural data from concentrated solutions of PE-stars or brushes can be fitted.

## Conclusions

We have presented a simple, mean-field model that describes the electrosteric interaction between spherical polyelectrolyte brushes. In this way the present model completes the theory of steric interaction that was first considered for uncharged systems by Fischer nearly 50 years ago [5]. The model predicts the values of the osmotic coefficient as a function of the physical properties of the spherical brush. It reproduces the experimental finding of the insensitivity of the coefficient to the concentration of the solution. At this stage, the values of the coefficients are still too low when compared with the experimental values, however [15]. Because the fraction of free counterions is very small anyway, this discrepancy does not have any serious consequences on the form and the quantitative characteristics of the effective interaction potential $V_{\rm eff}(D)$. $V_{\rm eff}(D)$ has been shown to have the form of an ultrasoft repulsion the range of which is set by the spatial extent of the spherical brush.

In general, such ultrasoft pair potentials lead to a rich phase behavior of the underlying physical systems. Unusual phase behavior, such as re-entrant melting and exotic crystal phases, such as body-centered orthogonal (bco), hexagonal, trigonal, and diamond lattices have been theoretically predicted for such diverse systems as neutral stars [10], ionic microgels [29], and PE-stars (unpublished work). It is therefore justified to expect similar exotic structural correlations also for spherical PE-brush solutions. This requires and deserves a further detailed study.

## References

1. Distler D (1999) Waessrige Polymerdispersionen. Wiley–VCH, New York
2. Russel WB, Saville DA, Schowalter WR (1989) Colloidal dispersions. Cambridge University Press, Cambridge
3. Napper DH (1989) Polymeric stabilization of colloidal dispersions. Academic Press, London
4. Iraelachvili J (1992) Intermolecular and surfaces forces, 2nd edn. Academic Press, London
5. Fischer EW (1958) Kolloid Zeitschr 160:120
6. Fleer GJ, Cohen Stuart MA, Scheutjens JMHM, Cosgrove T, Vincent B (1993) Polymers at interfaces. Chapman and Hall, London
7. Witten TA, Pincus PA (1986) Macromolecules 19:2509
8. Likos CN, Löwen H, Watzlawek M, Abbas B, Jucknischke O, Allgaier J, Richter D (1998) Phys Rev Lett 80:4450
9. Jusufi A, Watzlawek M, Löwen H (1999) Macromolecules 32:4470
10. Watzlawek M, Likos CN, Löwen H (1999) Phys Rev Lett 82:5289
11. Jusufi A, Likos CN, Löwen H (2002) Phys Rev Lett 88:018301
12. Jusufi A, Likos CN, Löwen H (2002) J Chem Phys 116:11011
13. Dingenouts N, Merkle R, Guo X, Narayan T, Goerick G, Ballauff M (2003) J Appl Crystallogr 36:578
14. Guo X, Ballauff M (2001) Phys Rev E 64:051406
15. Das B, Guo X, Ballauff M (2003) Progr Colloid Polym Sci 121:34
16. Klein Wolterink J, Leermakers FAM, Fleer GJ, Koopal LK, Zhulina EB, Borisov OV (1999) Macromolecules 32:2365
17. Winkler RG, Gold M, Reineker P (1998) Phys Rev Lett 80:3731
18. Nyquist RM, Ha B-Y, Liu A (1999) Macromolecules 32:3481
19. Jiang J, Liu H, Hu Y (1999) J Chem Phys 110:4952
20. Manning GS (1969) J Chem Phys 51:924
21. Odijk T, Houwaart AH (1978) J Polym Sci Polym Phys 16:627
22. Deserno M, Holm C, May S (2000) Macromolecules 33:199
23. Hansen J-P, Löwen H (2000) Ann Rev Phys Chem 51:209
24. Likos CN (2001) Phys Rep 348:267
25. Alexander S (1977) J Phys Paris 38:983
26. de Gennes P-G (1980) Macromolecules 13:1069
27. Milner ST, Witten TA, Cates ME (1988) Macromolecules 21:2610
28. Pincus P (1991) Macromolecules 24:2912
29. Gottwald D, Likos CN, Kahl G, Löwen H (2004) Phys Rev Lett 92:068301